Journal of The Electrochemical Society, 2021 **168** 036514
1945-7111/2021/168(3)/036514/13/$40.00 © 2021 The Electrochemical Society ("ECS"). Published on behalf of ECS by IOP Publishing Limited

Altering Electronic and Optical Properties of Novel Benzothiadiazole Comprising Homopolymers via π Bridges

Cansu Zeytun Karaman,[1] Seza Göker,[2] Serife O. Hacioğlu,[3] Tuğba Hacıefendioğlu,[1] Erol Yıldırım,[1,4] and Levent Toppare[1,4,5,z]

[1]*Chemistry Department, Middle East Technical University, Ankara 06800, Turkey*
[2]*Solid Propellant Department, Roketsan Missiles Inc., Ankara 06500, Turkey*
[3]*Department of Engineering Basic Sciences, Iskenderun Technical University, Iskenderun 31200, Turkey*
[4]*Department of Polymer Science and Technology, Middle East Technical University, Ankara 06800, Turkey*
[5]*The Center for Solar Energy Research and Application (GUNAM), Middle East Technical University, Ankara 06800, Turkey*

Four novel benzo[c][1,2,5]thiadiazole comprising monomers namely 5-fluoro-6-((2-octyldodecyl)oxy)-4,7-di(thiophen-2-yl)benzo[c][1,2,5]thiadiazole (TBTT), 5-fluoro-4,7-bis(4-hexylthiophen-2-yl)-6-((2-octyldodecyl)oxy)benzo[c][1,2,5]thiadiazole (HTBTHT), 5-fluoro-4,7-di(furan-2-yl)-6-((2-octyldodecyl)oxy)benzo- [c][1,2,5]thiadiazole (FBTF), and 5-fluoro-6-((2-octyldodecyl)oxy)-4,7-bis(thieno[3,2-b]thiophen-2-yl)benzo[c][1,2,5]thiadiazole (TTBTTT) were designed, and synthesized successfully via Stille polycondensation reaction. The structural characterizations of the monomers were performed by ^{1}H and ^{13}C NMR spectroscopy and High Resolution Mass Spectroscopy (HRMS). The monomers were then electropolymerized in a three electrode cell system via cyclic voltammetry. The electrochemical, and spectroelectrochemical characterization of the polymers were reported in detail. Besides, theoretical calculations were performed to elucidate observed experimental properties. According to the cyclic voltammogram of the polymers, HOMO and LUMO energy levels were calculated as −5.68 eV/−3.91 eV, −5.71 eV/−3.72 eV, −5.61 eV/−4.04 eV, and −5.51 eV/−3.71 eV and the electronic band gaps were 1.77 eV, 1.99 eV, 1.57 eV, and 1.80 eV for PTBTT, PHTBTHT, PFBTF, and PTTBTTT, respectively.
 [DOI: 10.1149/1945-7111/abedc5]

Manuscript submitted January 18, 2021; revised manuscript received March 3, 2021. Published March 22, 2021.

Supplementary material for this article is available online

Conjugated conductive polymers are organic semiconductors composed of alternating single and double bonds in their skeletons.[1] In recent years, these macromolecules received remarkable attention from both academic and industrial communities since they can be applied in many interdisciplinary fields such as photovoltaic devices (OPVs), electrochromics (EDCs), organic light-emitting diodes (OLEDs), biosensors, and organic field-effect transistors (OFETs).[2–8] Besides, they exhibit useful features over their silicon-based counterparts like easy processing, being flexible, having low-cost, ease of structural modifications.[9–11] There are a number of structural modifications for conjugated polymers (CPs) that can alter aromaticity, bond length alternation, interchain interaction, and planarity.[12–15] However, the donor-acceptor (D-A) concept can be considered as one of the most critical modifications in order to tune the band gap of the CPs.[16] In literature, thienopyrroledione (TPD), diketopyrrolopyrrole (DPP), benzooxadiazole (BO), benzotriazole (BTz), and benzothiadizole (BT)[17–21] are classified as the most used electron-withdrawing aromatic heterocycles. Lately, benzothiadiazole gains significant attention due to its comprising strong electron-accepting sulfur atom and two imine (−C=N−) bonds in its skeleton.[22] Besides, it also plays a significant role in obtaining a narrow band gap CPs. The electron-accepting ability of the benzothiadiazole can be improved by the introduction of fluorine atom to the backbone since it is the most electronegative atom and the smallest electron-withdrawing group. Therefore, the replacement of the hydrogen atom with fluorine atom does not create any steric hindrance.[23] Moreover, fluorinated BT units provide lower HOMO-LUMO energy levels, which presents better oxidative and thermal stabilities compared to their nonfluorinated BT counterparts.[24] In addition, the introduction of alkoxy unit with a long-branched alkyl chain increases both solubility and molecular weight of the polymer of BT acceptor.[25] Via these modifications, benzothiadiazole can be one of the strongest candidates for D-A type polymers. In literature, thiophene, 3-hexylthiophene, thieno[3,2-b]thiophene, and furan[26–29] are the most popular electron-donating units in A-D type CPs. Among them, thiophene is the popular one since it provides narrow band gap polymers with high charge carrier mobility and intermolecular interactions.[30] The effect of alkyl chain substituted thiophenes like 3-hexylthiophene (HT) are not much explored yet. However, HT provides unique optical and electronic behaviors on the polymer skeleton. Besides, it presents better solubility and processibility due to its alkyl chain.[31] Unlike thiophene and 3-hexylthiophene, thieno[3,2-b]thiophene exhibits different properties due to higher delocalization of the electrons along the backbone. With the extended conjugation and planarity, the narrower band gap and larger absorption spectrum could be obtained. Besides, it provides an enhanced intermolecular charge-carrier hopping mechanism.[32] Furan is another strong donor unit since the oxygen atom of the furan makes various contributions to optical and electronic properties of the polymer. It has higher electronegativity and smaller atomic size than its sulfur counterpart. Therefore, furan-based polymers exhibit lower steric hindrance and better aromaticity on polymer backbone.[33] Furthermore, Sotzing et al. synthesized a furan comprising polymer via electropolymerization, and the polymer presents a low band gap of 1.04 eV and a stable oxidation-reduction (redox) behavior.[34] In this work, a series of thiophene, 3-hexylthiophene, thieno[3,2-b]thiophene, and furan comprising novel copolymers were synthesized. The effect of donor units was explored by electrochemical and spectroelectrochemical characterizations and supported by computational studies.

Experimental

General.—For the synthesis, all the chemicals were purchased from Sigma-Aldrich except that 4,5-difluoro-2-nitroaniline was purchased from Tokyo Chemical Industry (TCI). Dry solvents were dispensed from a MB-SPS-800 solvent drying system. Column chromatography was run by using Merck Silica Gel 60 with the pore size 0.040–0.063 mm. Homopolymerization of the monomers was performed by electropolymerization in a three-electrode cell system. These electrodes were platinum wire as the counter electrode, the silver wire used as the reference electrode, and Indium Tin Oxide (ITO) coated glass as the working electrode. All electrochemistry studies were run by using GAMRY Reference 600 potentiostat. Electropolymerization performed in 0.1 M acetonitrile/dichloromethane solvent couple containing tetrabutylammonium

[z]E-mail: toppare@metu.edu.tr

tetrafluoroborate as the supporting electrolyte. Cyclic voltammetry studies were used to determine oxidation and reduction potentials. Perkin Elmer Lambda 25 UV/Vis Spectrometer was utilized to determine spectroelectrochemical features. Bruker Spectrospin Avance DPX-400 Spectrometer assigned the ^{1}H and ^{13}C of the synthesized chemicals (Scheme 1). HRMS measurements were performed by Waters Synapt G1 High Definition Mass Spectrometer.

Computational methods.—Theoretical calculations were carried out for tetramers of PTBTT, PHTBTHT, PFBTF and PTTBTTT in the form of DADADADA (D: donor, A: acceptor) by using B3LYP hybrid functional and 6–311 G(d) basis set with tight SCF convergence criteria in the Gaussian09 (Revision A.02) software package.[35–37] Adequate agreement was achieved with experimental results previously at this level of calculations for donor-acceptor copolymer studies.[38–40] Alkyl side chains on the polymers were replaced with ethyl groups to increase computational efficiency. Geometry optimizations were started from different initial conformations by controlling the torsional angle between connected donor and acceptor units to determine lowest energy geometry. Electrostatic potential surface (ESP), highest occupied molecular orbitals (HOMO), and lowest unoccupied molecular orbitals (LUMO) were calculated for the optimized geometries of tetramers. Band gap was calculated by using two different methods that are direct difference between the HOMO energy and LUMO energy for the optimized ground state and the calculation vertical excitation energy of the lowest singlet excited state ($S_0 \rightarrow S_1$). The singlet excited states of the oligomers were calculated by using time-dependent density-functional theory (TDDFT) at the same level of calculation quality. Vertical ionization potential (VIP) and adiabatic ionization potential (AIP) were calculated by the energy difference between the neutral tetramer and cation state of the optimized ground state geometry, followed by optimized cation geometry, respectively. Hole reorganisation energies (λreorg) were determined based on the formulation by Bredas et al.[41] Atomic charges were calculated based on the ESP fitting scheme of Merz-Singh-Kollman (MK).[42]

Synthesis of 4,5-difluorobenzene-1,2-diamine.—4,5-Difluoro-2-nitroaniline (1.25 g, 7.18 mmol) and 12 M HCl (30 ml) were mixed under nitrogen atmosphere. The reaction medium was cooled to 0 °C, and tin powder (4.13 g, 34.8 mmol) was added in three portions. After the depletion of tin powder at room temperature, reaction mixture was poured into 100 ml of distilled water. Then, NaOH was added until adjusting pH to 10. The organic layer was extracted with ethyl acetate and washed with brine and distilled water. The organic layers were combined and dried over anhydrous $MgSO_4$. After removal of solvent by rotary evaporation, the white cotton solid was obtained. The yield was 78%.^{1}H NMR (400 MHz, $CDCl_3$) δ 6.51 (t, J = 9.5 Hz, 2H), 3.28 (s, 4H). ^{13}C NMR (100 MHz, $CDCl_3$) δ 145.2, 145.0, 142.8, 142.6, 130.6, 130.5, 105.4, 105.3, 105.3, 105.2.

Synthesis of 5,6-difluorobenzo[c][1,2,5]thiadiazole.—4,5-Difluorobenzene-1,2-diamine (1.70 g, 11.8 mmol) and triethylamine (6.58 ml, 47.2 mmol) were dissolved in 60 ml of $CHCl_3$ in a two-necked flask under inert atmosphere. When reaction mixture was cooled to 0 °C, $SOCl_2$ (1.72 ml, 23.6 mmol) was added dropwise and

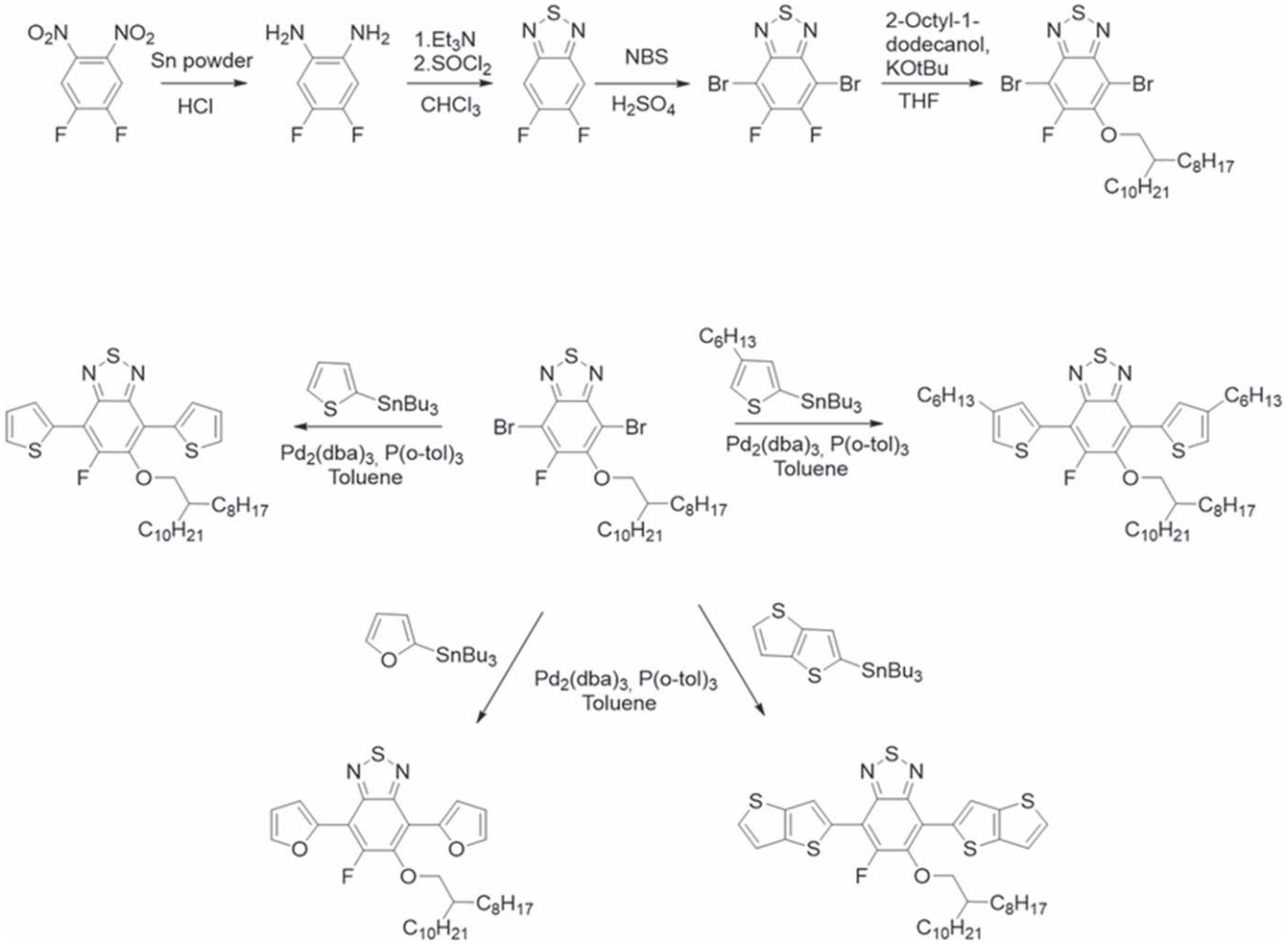

Scheme 1. Synthetic route for monomers.

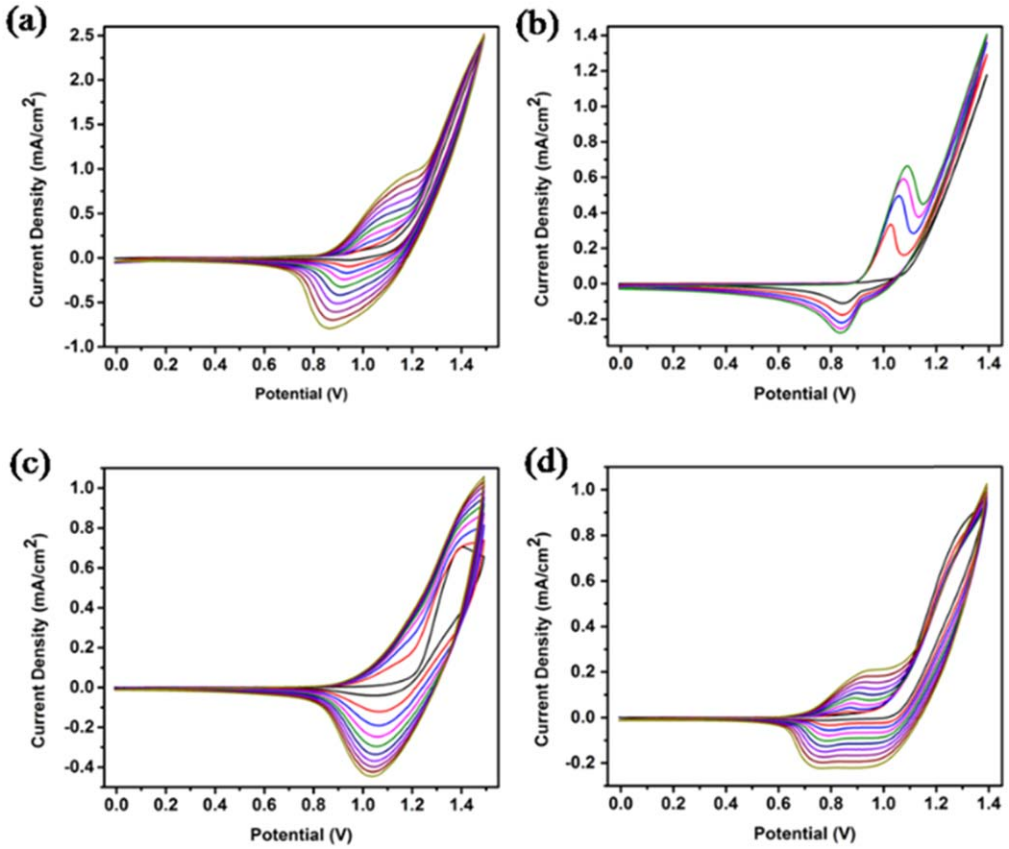

Figure 1. Electrochemical deposition of (a) PTBTT (b) PHTBTHT (c) PFBTF and (d) PTTBTTT on ITO coated glass slides in 0.1 M $TBABF_4$/DCM/ACN solution at a scan rate of 100 mV s^{-1}.

the mixture was heated to reflux for 5 h. The organic layer was washed with water and dried over $MgSO_4$. After removal of the solvent under reduced pressure, a brown solid was obtained. The yield was 63%. ^{1}H NMR (400 MHz, $CDCl_3$) δ 7.75 (t, J = 8.7 Hz, 2H). ^{13}C NMR (100 MHz, $CDCl_3$) δ 155.08 (d, J = 19.9 Hz), 152.49 (d, J = 20.0 Hz), 150.82 (t, J = 5.5 Hz), 106.11 (dd, J_1 = 14.8, J_2 = 6.8 Hz). ^{13}C NMR (100 MHz, CDCl3) δ 153.0, 152.8, 150.4, 150.2, 148.7, 148.7, 99.3, 99.2, 99.2, 99.1.

Synthesis of 4,7-dibromo-5,6-difluorobenzo[c][1,2,5]thiadiazole.—5,6-Difluorobenzo[c][1,2,5]thiadiazole (3.88 g, 22.5 mmol) was dissolved in 100 ml concentrated H_2SO_4 in a two-necked flask. Then, n-bromosuccinimide (16.05 g, 90.15 mmol) was added in three portions. The reaction mixture was stirred and heated to 70 °C for 8 h under a dark medium. After cooling to room temperature, the reaction mixture was poured into an ice-water mixture to afford a white precipitate. The solid was filtered and washed with water and allowed to dry. With the evaporation of residual solvent, the solid was recrystallized in methanol and a white wool product was obtained. The yield was 41%. ^{13}C NMR (100 MHz, $CDCl_3$) δ 153.0, 152.8, 150.4, 150.2, 148.7, 148.7, 99.3, 99.2, 99.2, 99.1.

Synthesis of 4,7-dibromo-5-fluoro-6-((2-octyldodecyl)oxy)benzo[c][1,2,5]thiadiazole.—4,7-Dibromo-5,6-difluorobenzo[c][1,2,5]thiadiazole (0.70 g, 2.12 mmol), 2-octyl-1-dodecanol (3.78 ml, 10.6 mmol) and KOtBu (0.21 g, 1.9 mmol) were dissolved in 40 ml dry THF under argon atmosphere. The reaction mixture was stirred and heated to reflux for overnight. Through evaporation of the solvent under reduced pressure, the crude product was washed with water and the organic layer was extracted dichloromethane. Organic phases were collected and dried with $MgSO_4$. After removal of the solvent, the liquid product was prufied by column chromatography on silica gel using 1.5:1 dichloromethane:hexane.The yield was 87%. ^{1}H NMR (400 MHz, $CDCl_3$) δ 4.12 (d, J = 5.1 Hz, 2H), 1.90–1.68 (m, 1H), 1.59 (m, J = 10.0, 4.8 Hz, 2H), 1.28 (m, J = 12.4 Hz, 30H), 0.87 (m, J = 2.1 Hz, 6H). ^{13}C NMR (100 MHz, $CDCl_3$) δ 157.9, 155.3, 150.0, 149.6, 149.4, 149.0, 149.0, 105.9, 105.8, 98.6, 98.4, 78.1, 78.0, 39.1, 31.9, 31.9, 31.0, 29.9, 29.6, 29.6, 29.6, 29.3, 29.3, 26.8, 22.6.

Synthesis of tributyl(thiophen-2-yl)stannane.—In a three-necked round bottom flask, thiophene (2.00 g, 23.8 mmol) was dissolved in freshly distilled THF under argon atmosphere. The reaction medium was cooled to −78 °C, and n-butyl lithium (1.67 g, 2.5 M in hexane, 26.2 mmol) was added drop wise. This solution was stirred for 2 h under inert atmosphere at the same temperature. Then tributyltin chloride (7.09 ml, 26.2 mmol) was added drop wise. Reaction mixture was allowed to reach room temperature and stirred for overnight. After removal of the solvent under reduced pressure, the organic layer was extracted with dichloromethane and washed with brine and water three times. Organic phases were combined and dried distilled over $MgSO_4$. The product was concentrated on rotary evaporator and light-yellow liquid was obtained as the product. The yield was 85%. ^{1}H NMR (400 MHz, $CDCl_3$) δ 7.57 (d, J = 4.7 Hz, 1H), 7.20–7.17 (t, J = 3.3 Hz 1H), 7.12 (d, J = 3.2 Hz, 1H), 1.49 (m, J = 15.8, 8.2 Hz, 6H), 1.27 (t, J = 14.7, 6H), 1.11–0.97 (m, 6H), 0.82 (t, J = 7.3 Hz, 9H). ^{13}C NMR (100 MHz, $CDCl_3$) δ 136.1, 135.1, 130.5, 127.8, 28.9, 28.8, 27.5, 27.2, 13.6.

Synthesis of 5-fluoro-6-((2-octyldodecyl)oxy)–4,7-di(thiophen-2-yl)benzo[c][1,2,5]thiadiazole.—4,7-Dibromo-5-fluoro-6-((2-octyldodecyl)oxy)benzo[c][1,2,5]thiadiazole (0.6 g, 0.97 mmol) and 2-(tributylstannyl)thiophene (0.81 g, 2.17 mmol) were dissolved in 40 ml dry toluene and stirred under argon atmosphere for 1 h. Then, bis(dibenzylideneacetone) palladium (0) (44.00 mg, 48.00 μmol) and tri(o-tolyl)phosphine (60.00 mg, 0.19 mmol) were added and the mixture was heated to 110 °C for 2 d under inert atmosphere. The product was concentrated on

rotary evaporator and the solid product was purified by column chromatography on silica gel using eluent 1:5 dichloromethane: hexane.The yield was 33%. ^{1}H NMR (400 MHz, $CDCl_3$) δ 8.41 (d, J = 3.8 Hz, 1H), 8.27 (d, J = 3.7 Hz, 1H), 7.58 (d, J = 5.2 Hz, 1H), 7.53 (d, J = 5.2 Hz, 1H), 7.24 (m, J_1 = 7.0 Hz, J_2 = 3.0 Hz, 2H), 4.00 (d, J = 5.9 Hz, 2H), 1.99–1.93 (m, 1H), 1.57–1.47 (m, 4H), 1.27 (s, 28H), 0.88 (s, 6H). ^{13}C NMR (100 MHz, $CDCl_3$) δ 156.2, 153.6, 150.3, 149.5, 149.4, 147.1, 146.9, 133.3, 133.3, 132.2, 132.1, 130.8, 130.4, 130.3, 128.1, 128.0, 127.8, 127.1, 126.8, 117.3, 111.6, 111.4, 77.8, 39.0, 31.9, 31.0, 30.0, 29.7, 29.4, 26.7, 22.7, 14.1. HRMS (ESI, m/z), $[M + H]^+$: for $C_{34}H_{48}N_2OFS_3$, calculated 615.2913 found 615.2914.

Synthesis of tributyl(4-hexylthiophen-2-yl)stannane.—In a three-necked round bottom flask, 3-hexylthiophene (2.50 g, 14.9 mmol) was dissolved in freshly distilled THF under argon atmosphere. The reaction medium was cooled to −78 °C, and n-butyl lithium (6.54 ml, 2.5 M in hexane, 16.3 mmol) was added drop wise. This solution was stirred for 2 h under inert atmosphere at the same temperature. Then tributyltin chloride (4.43 ml, 16.3 mmol) was added drop wise. Reaction mixture was allowed to reach room temperature and stirred for overnight. After removal of the solvent under reduced pressure, the organic layer product was extracted with dichloromethane and washed with brine and distilled water three times. Organic phases were combined and dried over $MgSO_4$. The product was concentrated on rotary evaporator and light-yellow liquid was obtained as the product. The yield was 83%. ^{1}H NMR (400 MHz, $CDCl_3$) δ 7.20 (s, 1H), 6.98 (s, 1H), 2.70–2.62 (t, 2H), 1.69–1.61 (m, 8H), 1.60–1.53 (m, 10H), 1.37–1.31 (m, 8H), 1.13–1.06 (m, 9H), 0.91 (t, J = 7.3 Hz, 3H). ^{13}C NMR (100 MHz, $CDCl_3$) δ 144.4, 136.8, 136.2, 125.4, 31.7, 30.6, 29.9, 29.1, 28.9, 27.2, 22.6, 14.0, 13.6, 10.7.

Synthesis of 5-fluoro-4,7-bis(4-hexylthiophen-2-yl)-6-((2-octyldodecyl)oxy)benzo[c][1,2,5]thiadiazole.—4,7-Dibromo-5-fluoro-6-((2-octyldodecyl)oxy)benzo[c][1,2,5]thiadiazole (0.60 g, 0.97 mmol) and tributyl(4-hexylthiophen-2-yl)stannane (1.13 g, 2.47 mmol) were dissolved in 25 ml dry toluene and stirred under argon atmosphere for 1 h. Then, bis(dibenzylideneacetone)palladium (0) (44.4 mg, 0.48 mmol) and tri(o-tolyl)phosphine (60.0 mg, 0.19 mmol) were added and the mixture was heated to 110 °C for 2 d under inert atmosphere. The product was concentrated on rotary evaporator and the solid product was purified by column chromatography on silica gel using eluent 1:4 dichloromethane: hexane and the yield was 41%. ^{1}H NMR (400 MHz, $CDCl_3$) δ 8.25 (s, 1H), 8.10 (s, 1H), 7.17 (s, 1H), 7.12 (s, 1H), 3.99 (d, J = 6.0 Hz, 2H), 2.80–2.57 (m, 4H), 1.97 (m, J = 12.0, 6.2 Hz, 2H), 1.70 (m, J = 15.0, 7.4 Hz, 6H), 1.44–1.35 (m, 8H), 1.27 (s, 32H), 0.97–0.85 (m, 6H), 0.87 (m, J = 9.4, 7.4, 3.4 Hz, 6H). ^{13}C NMR (100 MHz, $CDCl_3$) δ 156.2, 153.6, 150.3, 149.5, 149.4, 147.0, 146.9, 143.3, 142.9, 133.1, 133.0, 132.2, 131.9, 131.8, 131.8, 131.7, 123.1, 123.0, 122.8, 117.3, 117.2, 111.5, 111.4, 77.8, 77.7, 39.1, 32.0, 31.8, 31.7, 31.0, 30.6, 30.5, 30.1, 29.8, 29.7, 29.7, 29.4, 29.2, 29.1, 26.8, 22.7, 22.7, 22.7, 14.1. HRMS (ESI, m/z), $[M + H]^+$: for $C_{46}H_{72}FN_2OS_3$, calculated 783.4791 found 783.4821.

Synthesis of 5-fluoro-4,7-di(furan-2-yl)-6-((2- octyldodecyl)oxy) benzo[c][1,2,5]thiadiazole.—4,7-Dibromo-5-fluoro-6-((2-octyldodecyl) oxy)benzo[c][1,2,5]thiadiazole (0.49 g, 0.81 mmol) and tributyl(furan-2-yl) stannane (0.64 ml, 2.01 mmol) were dissolved in 30 ml dry toluene and stirred under argon atmosphere for 2 h. Then, bis(dibenzylideneacetone) palladium (0) (40.00 mg, 40.00 μmol) and tri(o-tolyl)phosphine (0.05 g, 0.16 mmol) were added and the mixture was heated to 110 °C for 2 d under inert atmosphere. The product was concentrated on rotary evaporator and the solid product was purified by column chromatography on silica gel using eluent 1:6 dichloromethane: hexane. The yield 70%. ^{1}H NMR (400 MHz, $CDCl_3$) δ 7.74 (d, J = 0.8 Hz, 1H), 7.69 (d, J = 0.8 Hz, 1H), 7.52 (d, J = 3.3 Hz, 1H), 7.42 (d, J = 3.3 Hz, 1H), 6.66 (m, J = 7.6, 1.4 Hz, 2H), 4.02 (d, J = 5.6 Hz, 2H), 1.92–1.81 (m, 2H), 1.26 (s, 70 H), 0.88 (s, 6H). ^{13}C NMR (100 MHz, $CDCl_3$) δ 155.6, 153.0, 149.4, 148.1, 148.0, 147.4, 147.2, 146.9, 146.9, 145.8, 145.8, 143.5, 143.4, 143.0, 114.4, 114.3, 114.2, 113.7, 113.7, 111.7, 111.5, 108.2, 108.1, 78.0, 39.1, 31.7, 30.9, 29.9, 29.5, 29.5, 29.4, 29.2, 28.1, 27.7, 26.7, 26.6, 22.5, 17.3, 17.1, 13.9, 13.4. HRMS (ESI, m/z), $[M + H]^+$: for $C_{34}H_{48}N_2O_3FS$, calculated 583.3370 found 583.3370.

Synthesis of tributyl(thieno[3,2-b]thiophen-2-yl)stannane.—In a three-necked round bottom flask, thienothiophene (0.70 g, 4.99 mmol) was dissolved in freshly distilled THF under argon atmosphere. The reaction medium was cooled to −78 °C, and n-butyl lithium (2.20 ml, 2.5 M in hexane, 5.49 mmol) was added drop wise. This solution was stirred for 2 h under inert atmosphere at the same temperature. Then tributyltin chloride (1.80 g, 5.49 mmol) was added drop wise. Reaction mixture was allowed to reach room temperature and stirred for overnight. After removal of the solvent under reduced pressure, the organic layer was extracted with dichloromethane and washed with brine and distilled water three times. Organic phases were combined and dried over $MgSO_4$. The product was concentrated on rotary evaporator and light-yellow liquid was obtained as the product. The yield was 50%. ^{1}H NMR (400 MHz, $CDCl_3$) δ 7.38 (d, J = 5.0 Hz, 1H), 7.33 (s, J = 5.1 Hz, 1H), 7.23 (d, J = 5.2 Hz, 1H), 1.65–1.52 (m, 12H), 1.35 (m, J = 7.3 Hz, 6H), 1.19–1.08 (m, 6H), 0.90 (t, J = 7.3 Hz, 9H). ^{13}C NMR (100 MHz, $CDCl_3$) δ 136.0, 135.0, 130.4, 127.7, 28.8, 27.1, 13.5, 10.7.

Synthesis of 5-fluoro-6-((2-octyldodecyl)oxy)-4,7-bis(thieno[3,2-b]thiophen-2-yl)benzo[c][1,2,5]thiadiazole.—4,7-Dibromo-5-fluoro-6-((2-octyldodecyl)oxy)benzo[c][1,2,5]thiadiazole (0.50 g, 0.82 mmol) and tributyl(thieno[3,2-b]thiophen-2-yl)stannane (0.85 g, 2.05 mmol) were dissolved in 40 ml dry toluene and stirred under argon atmosphere for 1 h. Then, bis(dibenzylideneacetone) palladium (0) (37.5 mg, 0.81 mmol) and tri(o-tolyl)phosphine (50.0 mg, 0.41 mmol) were added and the mixture was heated to 110 °C for 2 d under inert atmosphere. The solution was concentrated on rotary evaporator and the solid product was purified by column chromatography on silica gel using eluent 1:4 dichloromethane: hexane. The yield was 50%. ^{1}H NMR (400 MHz, $CDCl_3$) δ 8.73 (s, 1H), 8.55 (s, 1H), 7.51–7.46 (m, 2H), 7.35–7.31 (m, 2H), 4.06 (d, J = 5.9 Hz, 2H), 2.05–1.99 (t, 1H), 1.56 (s, 4H), 1.27 (s, 28H), 0.89 (s, 6H). ^{13}C NMR (100 MHz, $CDCl_3$) δ 155.2, 152.6, 149.1, 148.3, 148.2, 146.0, 145.9, 140.7, 140.6, 138.5, 138.2, 134.4, 133.0, 127.8, 127.6, 122.2, 121.7, 121.6, 118.3, 116.6, 111.0, 110.8, 77.2, 38.0, 30.9, 29.9, 29.0, 28.7, 28.3, 25.7, 21.6, 13.1. HRMS (ESI, m/z), $[M + H]^+$: for $C_{38}H_{48}N_2OFS_5$, calculated 727.2354 found 727.2352.

Results and Discussion

Electrochemical studies.—Certain simplicity, easy use and multifunctionality of cyclic voltammetry (CV) make it a versatile and widely preferred technique for both electropolymerization and electrochemical characterization of the compounds.[43] Due to above-mentioned advantages all electrochemical polymerizations were performed via CV between 0.0 V and 1.4 V in 0.1 M acetonitrile (ACN)/dichloromethane (DCM) solvent couple (4/1, v/v) for PTBTT (1/1, v/v) for PHTBTHT and (1.5/1, v/v) for PFBTF and for PTTBTTT containing tetrabutylammonium tetrafluoroborate ($TBABF_4$) as the supporting electrolyte. The electropolymerization of the monomers were illustrated in Scheme 2. During electropolymerization, different solvent mixtures were used in order to improve the solubility of monomers and obtain a good polymer film formation on ITO coated glass electrodes. The voltammograms for electropolymerizations were depicted in Figs. 1a–1d. In addition, some crucial parameters such as oxidation/reduction potentials, HOMO/LUMO energy levels and electronic band gap (E_g^{el}) which

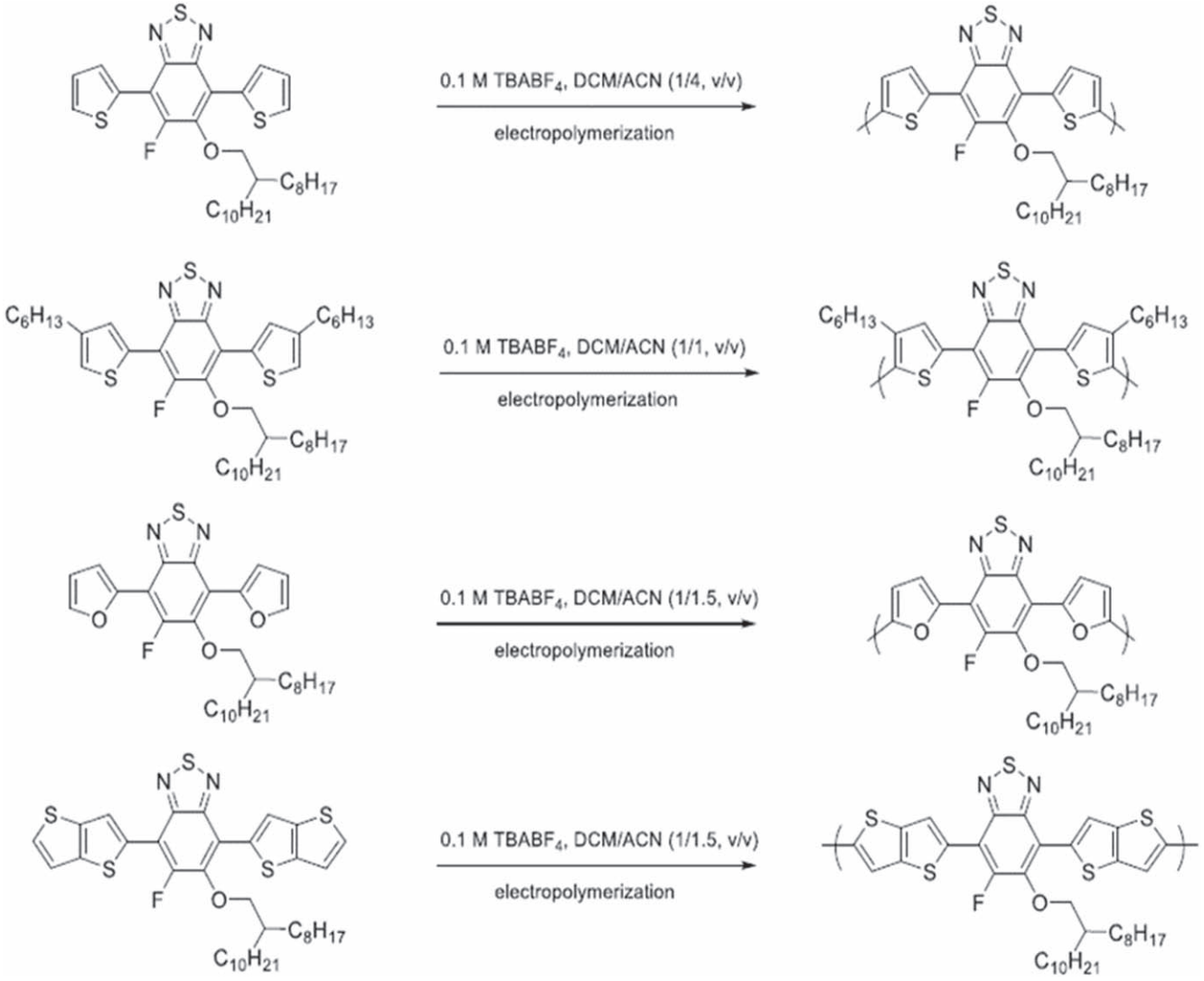

Scheme 2. Electropolymerization of monomers.

are vital for several of applications could be calculated from CV studies.

Figures 2a–2d show the single scan cyclic voltammograms (CVs) of electrochemically obtained polymers PTBTT, PHTBTHT, PFBTF and PTTBTTT. As seen in Fig. 2, thiophene and thienothiophene comprising polymers PTBTT and PTTBTTT exhibited ambipolar character (p-type and n-type doping behavior) with 1.17 V/−1.68 V and 1.03 V/−1.65 V oxidation and reduction potentials. However, 3-hexylthiophene and furan bearing polymers PHTBTHT and PFBTF showed only p-type doping behavior with 1.16 V and 1.33 V oxidation potentials.

After electrochemical syntheses, the redox behaviors of PTBTT, PHTBTHT, PFBTF and PTTBTTT were also investigated via CV in a three-electrode system (Ag wire as the reference electrode (RE), a Pt wire as the counter electrode (CE), and indium tin oxide (ITO)-coated glass slide as the working electrode (WE)) immersed in 0.1 M tetrabutylammonium hexafluorophosphate (TBAPF6)/acetonitrile (ACN) electrolyte/solvent couple at a scan rate of 100 mV s^{-1}.

When PTBTT, PHTBTHT, PFBTF and PTTBTTT were compared in terms of electrochemical behaviors as seen in Table I, thienothiophene comprising derivative PTTBTTT exhibited the lowest onset oxidation potential as 0.76 V which can be dedicated to the different electron densities of four donor groups (thiophene, 3-hexylthiophene, furan and thienothiophene), in other words, PTTBTTT has higher electron density with extended conjugation which results lower oxidation potential. The second lowest onset oxidation potential belongs to PFBTF with 0.86 V. This lower potential value is probably due to high electron density and high electron-donating ability of the furan. PTBTT and PHTBTHT show similar onset oxidation potentials at 0.93 V and 0.96 V, respectively.

HOMO/LUMO energy levels are also crucial parameters for polymers especially to determine their application fields and can be calculated from CVs. Herein, HOMO/LUMO energy levels of all polymers (PTBTT, PHTBTHT, PFBTF and PTTBTTT) were calculated from the onsets of the corresponding oxidation potentials and reported as −5.68 eV/−3.91 eV for PTBTT, −5.71 eV/−3.72 eV for PHTBTHT, −5.61 eV/−4.04 eV for PFBTF and −5.51 eV/−3.71 eV for PTTBTTT.

The scan rate dependences of the polymers (PTBTT, PFBTF and PTTBTTT) were studied by recording the single scan voltammograms at four different scan rates (50 mV s^{-1}, 100 mV s^{-1}, 150 mV s^{-1} in a monomer free 0.1 M $TBAPF_6$/ACN electrolyte solution. Current density—applied potential and current density—scan rate graphs were reported in Figs. 3 and 4. As seen, a linear

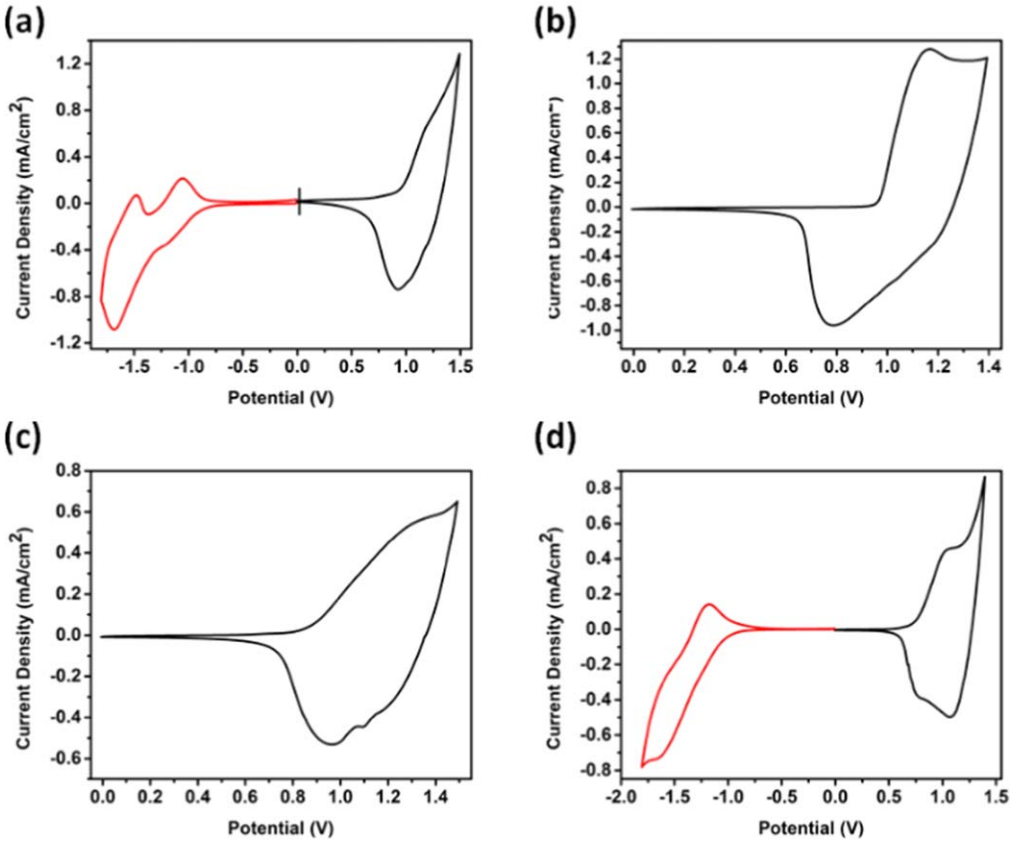

Figure 2. Single scan cyclic voltammograms of (a) PTBTT (b) PHTBTHT (c) PFBTF and (d) PTTBTTT in a monomer free 0.1 M $TBAPF_6$/ACN solution.

relationship between the current density and scan rate demonstrates the non-diffusion controlled mass transfer during doping—dedoping processes and formation of well adhered polymer films.

Spectroelectrochemical studies.—After electrochemical characterizations, UV–vis-NIR absorption spectra of the polymers were recorded in order to investigate the optical and electronic changes upon stepwise oxidation. Some crucial parameters like neutral state absorption maxima (λ_{max}), optical band gap (E_g^{op}) and polaronic region were calculated from UV–vis-NIR absorption spectra. Polymers were obtained electrochemically on ITO working electrode surface via CV as described before and spectroelectrochemical studies were performed in 0.1 M $TBAPF_6$/ACN solution using UV–vis-NIR spectrophotometer integrated with potentiostat. Initially, −0.5 V constant potentials were applied in order to record the true neutral film absorptions and then potential was sweeped between 0.0 V and 1.5 V for PTBTT, 0.0 V and 1.4 V for PHTBTHT, 0.0 V and 1.3 V for PFBTF and 0.0 and 1.4 V for PTTBTTT.

As seen in Figs. 5a–5d, the neutral state absorption maxima revealed at 549 nm for PTBTT, 511 nm for PHTBTHT, 592 nm for PFBTF and 536 nm for PTTBTTT which can be assigned to π–π^* transitions. Upon stepwise oxidation while the neutral state absorptions depleted, new absorption bands which correspond to the formation of radical cations (polaron bands) appeared at 805 nm for PTBTT, 840 nm for PHTBTHT, 875 nm for PFBTF and 770 nm for PTTBTTT, respectively. Another crucial parameter for conjugated polymers which affect their applicability in different fields like electrochromic devices, solar cells is the band gap (E_g) which can be calculated from the onset of the π–π^* transition of the neutral polymers films according to the equation $E_g^{op} = 1241/\lambda$. Band gaps were calculated as 1.65 eV (PTBTT), 1.99 eV (PHTBTHT), 1.57 eV (PFBTF) and 1.64 eV (PTTBTTT). All electrochemical and spectroelectrochemical analyses for all polymers (PTBTT, PHTBTHT, PFBTF and PTTBTTT) (Table I).

When spectroelectrochemical results were compared for all polymers (PTBTT, PHTBTHT, PFBTF and PTTBTTT) to get deep insight on the electron donor ability of thiophene, 3-hexylthiophene, furan and thienothiophene. As seen in Table I furan comprising PFBTF exhibited red shifted neutral state absorption centered at 592/652 nm with the lowest optical band gap calculated as 1.57 eV probably due to the better electron donor ability of furan unit as a π-bridge.[44] Even though PFBTF has the lowest E_g^{op}, a similar trend is not observed in E_g^{el}. This difference can be emerged from the formation of the charge on polymer film during the cyclic voltammetry run. Therefore, high E_g^{el} is resulted.[45] PTBTT and PTTBTTT have similar E_g^{op} values as 1.65 eV and 1.64 eV, respectively. Even though thiophene and thienothiophene have high electron densities and strong donating abilities, furan is more electronegative than its sulfur counterpart, so furan based polymers could reveal better properties. The highest E_g^{op} value belongs to PHTBTHT due to the bulky alkyl chain of the 3-hexylthiophene, which causes steric hindrance and interrupts coplanarity between aromatic rings on the polymer backbone. Therefore, distortion of the planarity results in higher E_g^{op}.[46]

As a further characterization, electrochromic properties of the resulting polymers were also investigated and all polymers exhibited a multichromic behavior which is important for variety of applications such as electrochromic devices, displays, mirrors, windows and sun-glasses.[47] Colors of all polymer films were recorded at different applied potentials and depicted in Figs. 6a–6d. As seen, the electrochromic properties and colors of the polymers in the neutral state are consistent with the neutral state absorption values. While the furan comprising polymer PFBTF with red shifted absorption (592/652 nm) exhibited bright blue color in the neutral state, the

Table I. Electrochemical and Spectroelectrochemical properties.

	E^{ox}_{mon} (V)	$E_{p\text{-doping}}^{onset}$ (V)	$E_{p\text{-doping}}$ (V)	$E_{p\text{-dedoping}}$ (V)	$E_{n\text{-doping}}$ (V)	$E_{n\text{-dedoping}}$ (V)	HOMO (eV)	LUMO (eV)	Λ_{max} (nm)	Λ_{max}^{onset} (nm)	E_g^{op} (eV)	Polaron (nm)
PTBTT	1.40	0.93	1.17	0.93	−1.20/ −1.68	−1.05/ −1.47	−5.68	−3.91	549	752	1.65	805
PHTBTHT	1.32	0.96	1.16	0.78	—	—	−5.71	−3.72	511	563	1.99	840
PFBTF	1.40	0.86	1.33	0.96	—	—	−5.61	−4.04	592/562	790	1.57	875
PTTBTTT	1.30	0.76	1.03	0.76	−1.65	−1.18	−5.51	−3.71	536	756	1.80	770

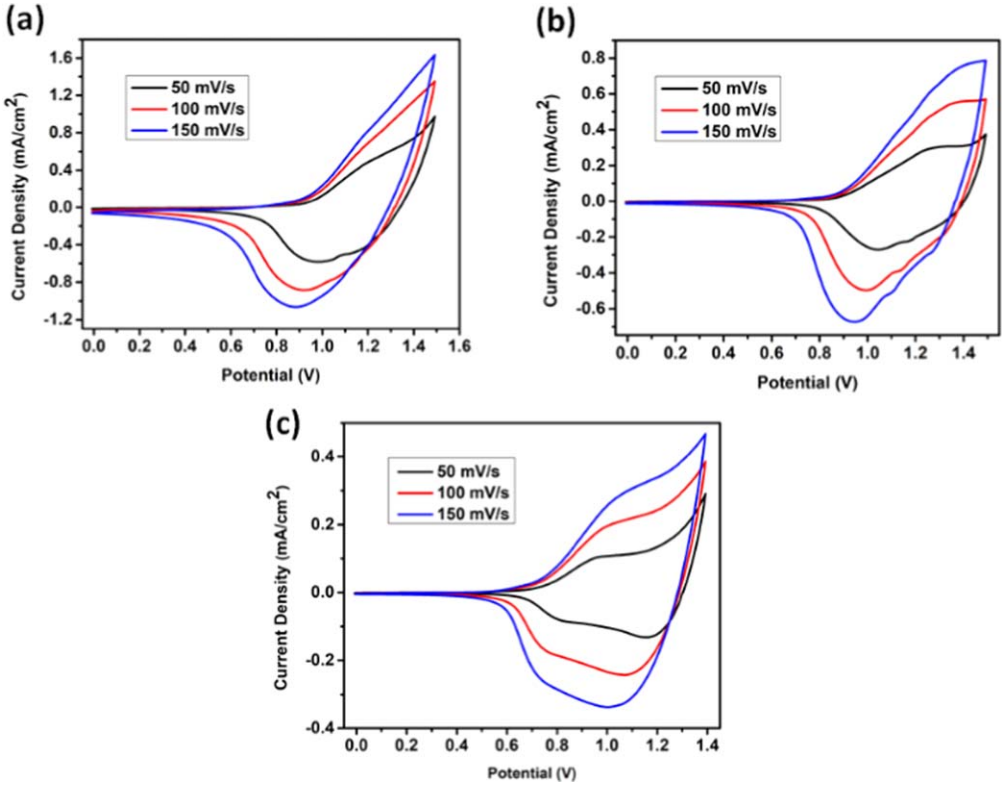

Figure 3. Scan rate dependence of (a) PTBTT (b) PFBTF and (c) PTTBTTT in 0.1 M $TBAPF_6$/ACN solution.

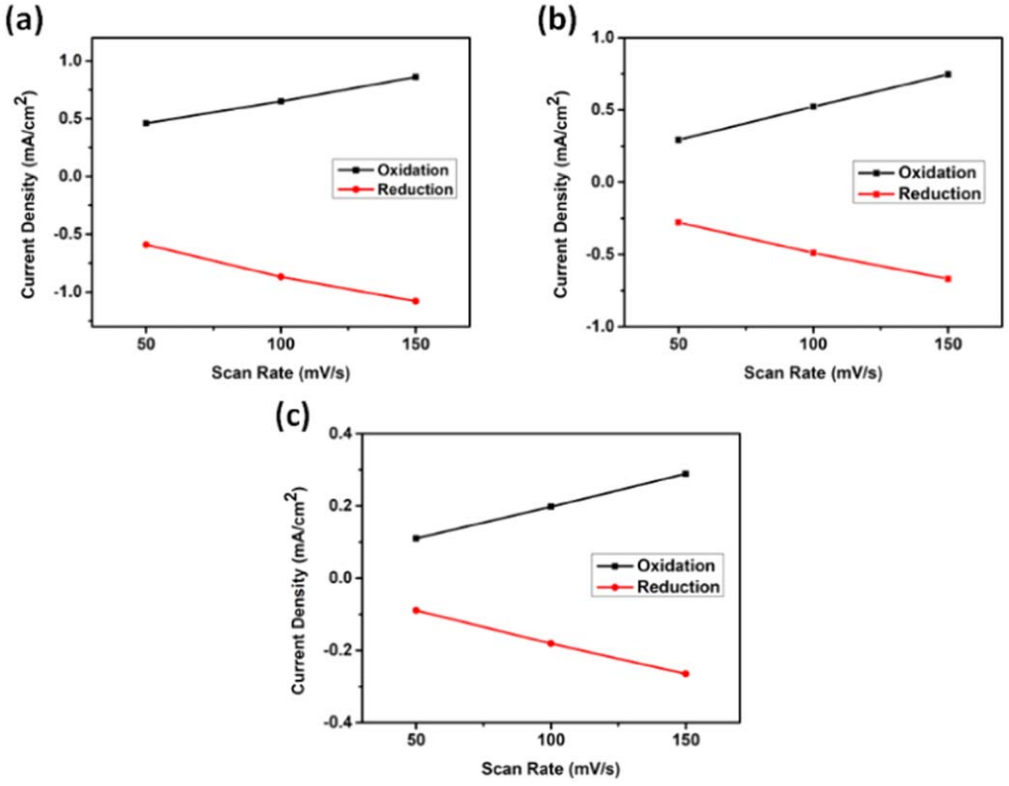

Figure 4. Current density—scan rate graphs of (a) PTBTT (b) PFBTF and (c) PTTBTTT in 0.1 M $TBAPF_6$/ACN solution.

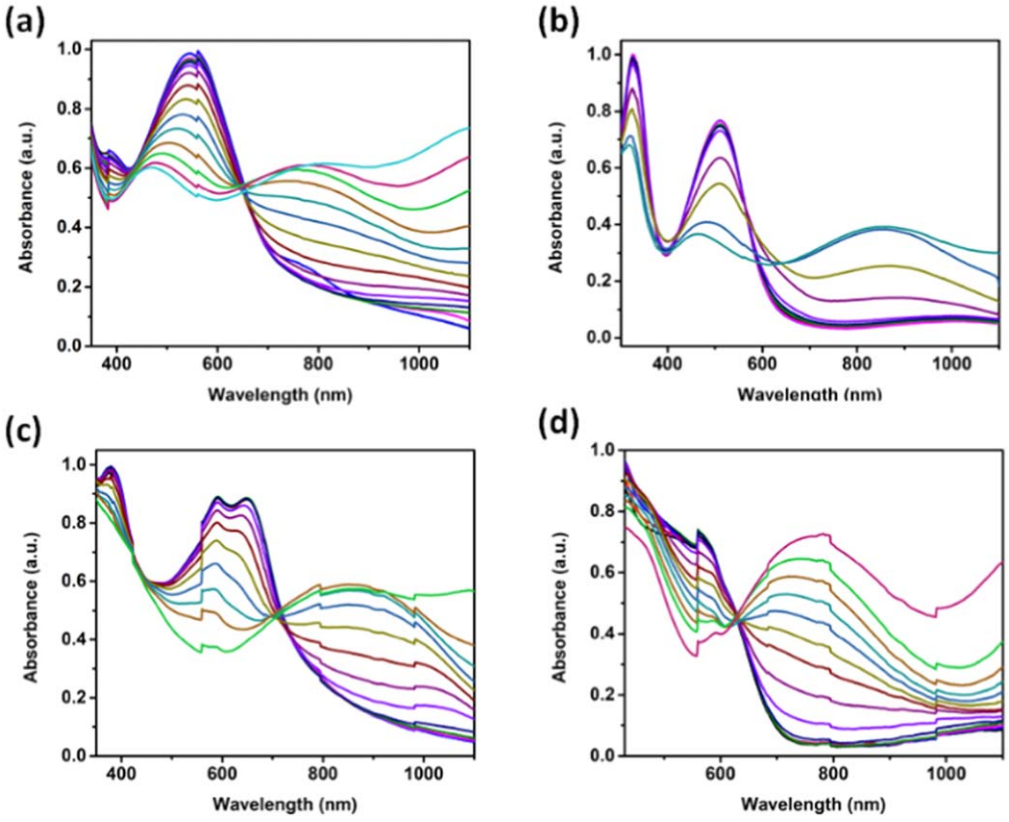

Figure 5. Electronic absorption spectra of all polymers in 0.1 M $TBAPF_6$/ACN solution between 0.0 V and 1.5 V for PTBTT, 0.0 V and 1.4 V for PHTBTHT, 0.0 V and 1.3 V for PFBTF and 0.0 and 1.4 V for PTTBTTT.

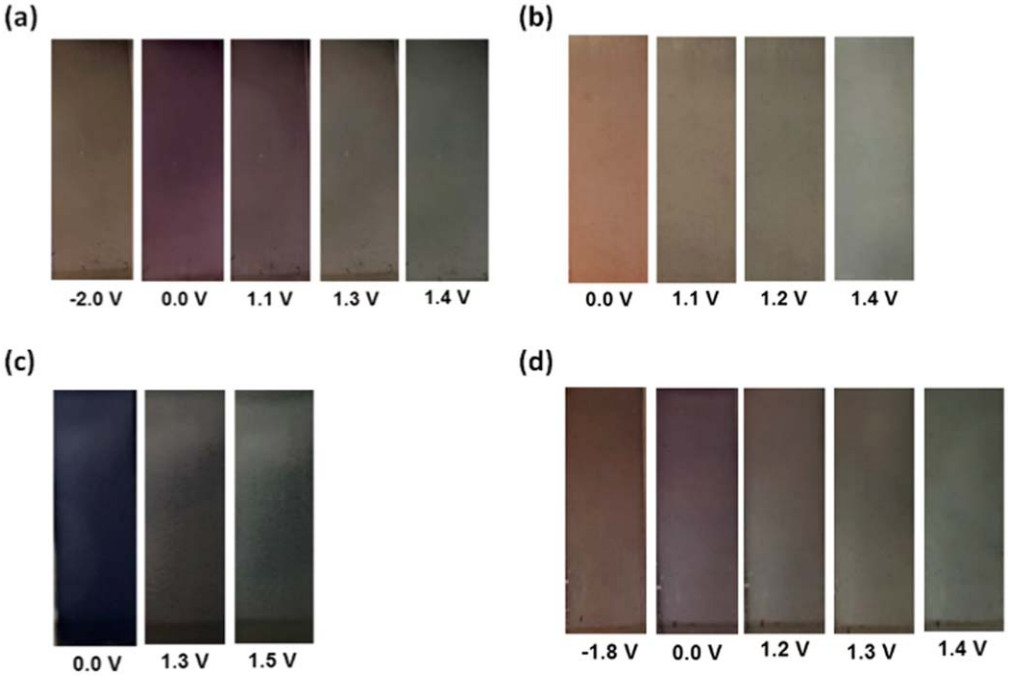

Figure 6. Colors of (a) PTBTT (b) PHTBTHT (c) PFBTF and (d) PTTBTTT at neutral and oxidized/reduced states.

bluest shifted (511 nm) polymer PHTBTHT exhibited orange color in the neutral state. In addition, PTBTT and PTTBTTT showed the different tones of red-purple in the neutral state with 549 nm and 536 nm absorption maxima. Furthermore, all polymers exhibited multi-electrochromic character and showed different tones of grayish green color in the oxidized states.

The thickness of the grown polymer film was an important parameter that can affect the spectroelectrochemical and electrochromic

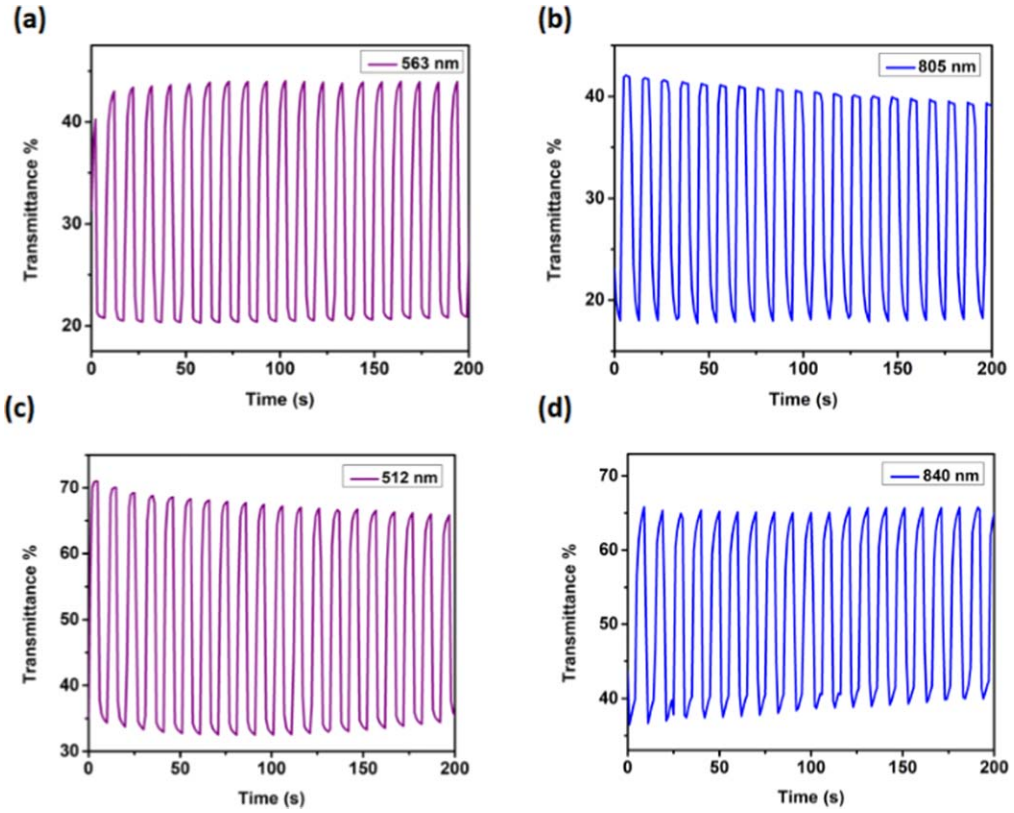

Figure 7. Electrochromic percent transmittance changes observed at the absorption maxima of (a,b) PTBTT and (c,d) PHTBTHT in 0.1 M $TBAPF_6$/ACN solution.

Table II. Kinetic properties of polymers.

	Λ_{max} (nm)	Optical Contrast (%)	Switching Time (s)
PTBTT	563	24	2.8
	805	24	2.1
PHTBTHT	512	37	2.1
	840	28	2.1
PFBTF	590	23	1.9
	915	11	1.8
PTTBTTT	570	26	2.3
	770	40	3.0

properties, and thickness values were calculated by using single scan cyclic voltammogram of the polymers. The thickness values of the polymer films were found as 77 nm, 95 nm, 54 nm, 65 nm for PTBTT, PHTBTHT, PFBTF, PTTBTTT, respectively.

Kinetic studies.—Kinetic studies were performed in order to explore and calculate the optical contrast (the change in percent transmittance) and switching time (the time required for coloring/bleaching processes between two extreme states) values while continuous stepping the potential between two extreme states (neutral and oxidized states) within 5 s time interval. The wavelengths used for the electrochromic switching studies were determined from the spectroelectrochemical studies as the maximum absorption wavelengths and reported in Table II. The percent transmittance-time graphs were displayed in Fig. 7 for PTBTT and PHTBTHT and in Fig. 8 for PFBTF and PTTBTTT and corresponding electrochromic switching properties were summarized in Table II.

As seen, the optical contrast values were measured as 24% (at 563 nm) and 24% (at 805 nm) for PTBTT and 37% (at 512 nm) and 28% (at 840 nm) for PHTBTHT from Fig. 7. Then, the optical contrast values were measured as 23% (at 590 nm) and 11% (at 915 nm) for PFBTF and 26% (at 570 nm) and 40% (at 770 nm) for PTTBTTT from Fig. 8.

As illustrated in Tables II, 3-hexylthiophene comprising polymer PHTBTHT exhibited the highest optical contrast as 37% in the visible region (at 512 nm). Finally, another important parameter namely switching time was calculated from Figs. 7 and 8 as 2.8 s and 2.1 s for PTBTT, 2.1 s and 2.1 s for PHTBTHT, 1.9 s and 1.8 s for PFBTF, 2.3 s and 3.0 s for PTTBTTT at the corresponding wavelengths.

Computational results.—HOMO, LUMO and ESP surfaces for the optimized geometries of tetramers of PTBTT, PHTBTHT, PFBTF and PTTBTTT are given in Fig. 9. HOMO orbitals were delocalized along the chain for tetramers instead for localizing on the donor acceptor. LUMO orbitals were also delocalized however less than HOMO, where they are mostly placed on the acceptor units as expected, especially on the central benzothiadiazole units. Relatively more disordered distribution of frontier orbitals was observed for PHTBTHT due to the higher nonplanarity compared to other copolymers. ESP surface shows well-ordered and sequential distribution of electron rich (red) donor and electron deficient (blue) acceptor sites. Significant effect of alkoxy and -F substitutions were observed on the electrostatic potential distribution of 5-fluoro-6-((2-octyldodecyl)oxy)benzo[c][1,2,5]thiadiazole acceptor unit where benzothiadiazole unit became more electron deficient, leading to the better acceptor properties due to these substitutions. Reduced regularity and reduced repeating patterns were observed for ESP of PHTBTHT due to its decreased planarity and electron conjugation.

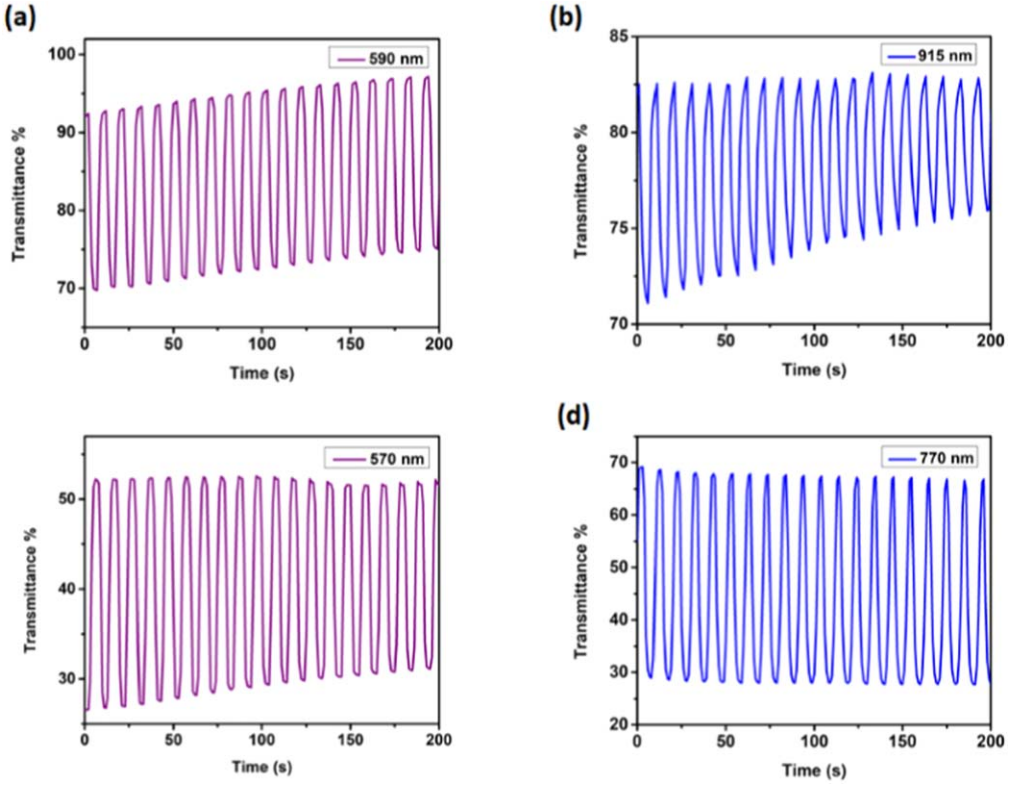

Figure 8. Electrochromic percent transmittance changes observed at the absorption maxima of (a,b) PFBTF and (c,d) PTTBTTT in 0.1 M $TBAPF_6$/ACN solution.

Table III. Electronic and structural properties of PTBTT, PHTBTHT, PFBTF and PTTBTTT by DFT method.

	θ D-A (eV)	θ D-D (eV)	VIP (eV)	AIP (eV)	λ_{reorg} (eV)	HOMO (eV)	LUMO (eV)	E_g^{el} (eV)	E_g^{op} (eV)	δ acceptor (eV)	δ donor (eV)
PTBTT	10.7 0.2	17.2	5.73	5.62	0.11	−5.07	−3.06	2.00	1.68	−0.39	0.21
PHTBTHT	11.9 0.7	68.3	6.04	5.82	0.21	−5.37	−2.85	2.52	2.13	−0.36	0.16
PFBTF	14.8 0.9	0.2	5.64	5.56	0.08	−4.94	−2.99	1.96	1.63	−0.97	0.49
PTTBTTT	9.6 0.5	19.3	5.60	5.52	0.08	−5.05	−3.13	1.92	1.61	−0.14	0.07

Torsional angles between donor and acceptor units are given in Table III. There are two types of angles due to the different substitutions on two carbon atoms at the two sides of benzothiadiazole unit. -F substitution did not disturb planarity and all the angles are below 1°.

However, alkoxy substitution significantly change planarity and torsional angles are between 9°–15°. Still the main reason for the difference in the planarity of the chains is the torsional angle between two connected donor units. The torsional angles between two donors of PHTBTHT is 68.3° due to the repulsions between alkyl groups which significantly reduce electronic and optical properties. The highest planarity was observed for PFBTF. Close values were determined three copolymers other than PHTBTHT, for the VIP, AIP and λ_{reorg} value which is directly related with the charge mobility. Ionization potentials agreed with the experimental results that show lowest values for PTTBTTT. Similarly, PTBTT, PFBTF and PTTBTTT show close optical and direct band gap values, with the exception of nonplanar PHTBTHT. The difference observed for experimental and computational band gap values are due to the interchain interactions that are not included in the theoretical calculations. Higher planarity of the PFBTF chains that leads to the better interchain packing resulted in the lower band compared to the single chain calculations and the most red-shifted neutral state absorption in the experiments. Finally, total average atomic charges (δ) by ESP fitting on the two donor and two acceptors in the middle of tetramers were calculated by neglecting end group donor-acceptor units to avoid end group effect. Although all copolymers have electron transfer from donor to acceptor according to these atomic charges, charge difference formed between donor and acceptor units are significantly higher in PFBTF which leads to the enhanced donor-acceptor capacity.

Conclusions

A novel 5-fluoro-6-((2-octyldodecyl)oxy)benzo[c][1,2,5]thiadiazole acceptor unit is coupled with donor units, namely, thiophene, 3-hexylthiophene, furan, and thieno[3,2-b]thiophene comprising monomers were synthesized and electropolymerized successfully. The theoretical studies showed that donors behave as good donors and acceptors behave as good acceptors. The electrochemical characterization of the polymers revealed that PTBTT and PTTBTTT are both p-type and n-type dopable. The electronic band gaps of the polymers were evaluated as 1.77, 1.99, 1.57 eV, and 1.80 eV for PTBTT, PHTBTHT, PFBTF, and PTTBTTT respectively. The band gap values are in between 1.00 eV and 2.00 eV, which means they are promising for organic solar cell applications. According to spectroelectrochemical characterizations, the most red-shifted neutral state absorption belongs to PFBTF. The colorimetry studies showed that the polymers exhibit

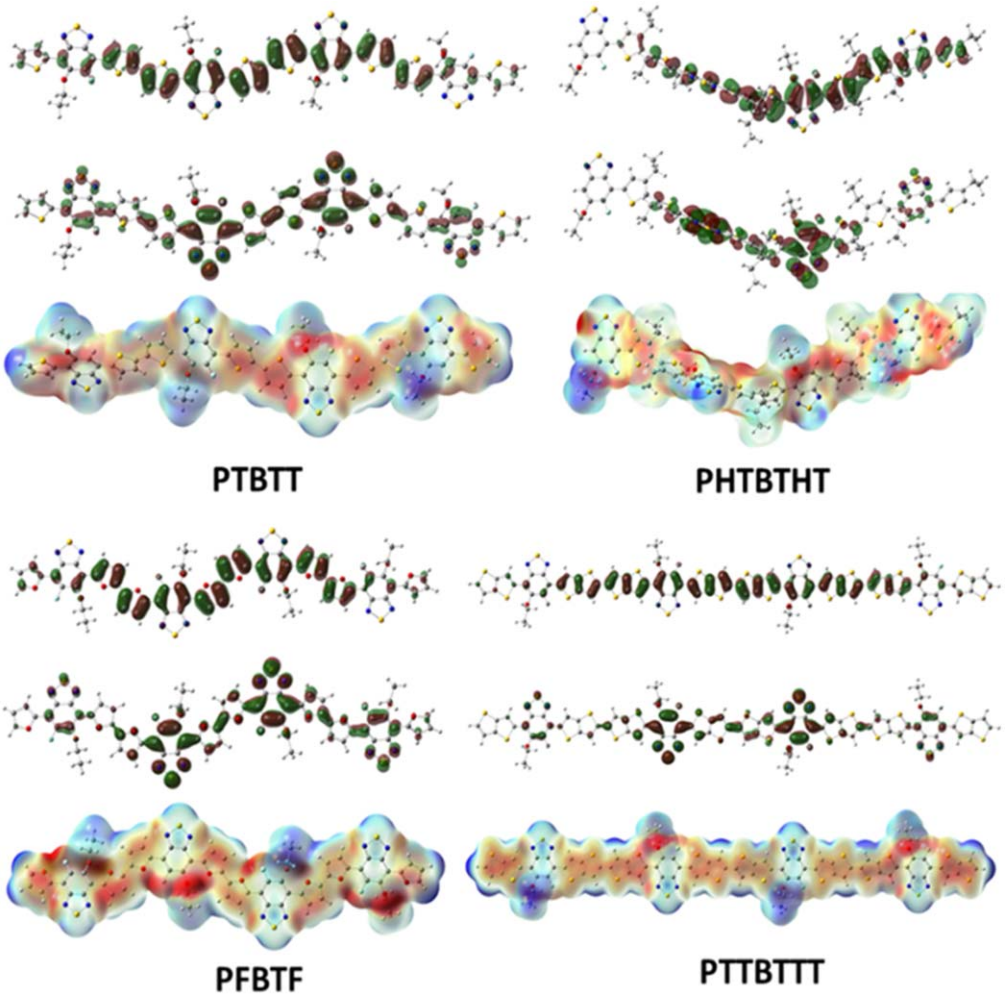

Figure 9. Molecular orbital surfaces of HOMO (top), LUMO (middle) and ESP mapping (bottom) for PTBTT, PHTBTHT, PFBTF and PTTBTTT.

multi electrochromic behavior in their neutral, oxidized, and reduced states. Therefore, they are also promising for electrochromic device applications. Results were discussed by comparing with the theoretical calculations.

Acknowledgments

The authors are thankful to METU Central Lab for HRMS results of the monomers. Erol Yıldırım gratefully acknowledges support from 2232 International Fellowship for Outstanding Researchers Program of TÜBİTAK (Project No: 118C251).

ORCID

Seza Göker https://orcid.org/0000-0002-0389-4260
Levent Toppare https://orcid.org/0000-0002-0198-4617

References

1. S. O. Hacioglu, D. Yiğit, D. Ermis, S. Soylemez, M. Güllü, and L. Toppare, *J. Electrochem. Soc.*, **163**, E293 (2016).
2. J. Xie, C. E. Zhao, Z. Q. Lin, P. Y. Gu, and Q. Zhang, *Asian J. Chem.*, **11**, 1489 (2016).
3. J. Du, M. Biewer, and M.-C. Stefan, *J. Mater. Chem. A*, **4**, 15771 (2016).
4. Y. Zhang, L. Kong, X. Ju, and J. Zhao, *Polymers*, **10**, 23 (2018).
5. I. Bala, R. A. K. Devi, J. De, N. Singh, K. Kailasam, and S. K. Pal, *J. Mater. Chem. C*, **8**, 17009 (2020).
6. S. Ramanavicius and A. Ramanavicius, *Polymers*, **13**, 49 (2021).
7. M. Barłóg, X. Zhang, I. Kulai, D.-S. Yang, D.-N. Sredojevic, A. Sil, and L. Fang, *Chem. Mater.*, **31**, 9488 (2019).
8. R. B. Song, Y. Wu, Z. Q. Lin, J. Xie, C. H. Tan, J. S. C. Loo, B. Cao, J. R. Zhang, J. J. Zhu, and Q. Zhang, *Angew. Chem. Int. Ed.*, **56**, 10516 (2017).
9. S. Soylemez, S. O. Hacioglu, S. D. Uzun, and L. Toppare, *J. Electrochem. Soc.*, **162**, H6 (2014).
10. J. Xie, Z. Wang, Z. J. Xu, and Q. Zhang, *Adv. Funct. Mater.*, **8**, 1703509 (2018).
11. C. J. Yao, H. L. Zhang, and Q. Zhang, *Polymers*, **11**, 107 (2019).
12. W. Huang, W. Xie, H. Huang, H. Zhang, and H. Liu, *J. Phys. Chem. Lett.*, **12**, 4548 (2020).
13. L. Dou, Y. Liu, Z. Hong, G. Li, and Y. Yang, *Chem. Rev.*, **115**, 12633 (2015).
14. J. Roncali, *Macromol. Rapid Commun.*, **28**, 1761 (2007).
15. N. M. Randell, C. L. Radford, J. Yang, J. Quinn, Y. Yang, D. Hou, Y. Li, and T. L. Kelly, *Chem. Mater.*, **30**, 4864 (2018).
16. N. E. Sparks, T. A. Ranathunge, N. H. Attanayake, P. Brodgon, J. H. Delcamp, R. G. Rajapakse, and D. L. Watkins, *ChemElectroChem*, **7**, 3752 (2020).
17. A. A. Advincula, I. Pelse, and J. R. Reynolds, *J. Mater. Chem. C*, **8**, 16452 (2020).
18. N. T. T. Truong, L. T. Nguyen, H. L. T. Mai, B. K. Doan, D. H. Tran, K. K. T. Truong, and V. M. Nguyen, *J. Polym. Res.*, **27**, 1 (2020).
19. R. Kottokkaran, A. Vishnumurthy, A. V. Kesavan, N. V. Vinila, and P. C. Ramamurthy, *Mater. Today Commun.*, **11**, 132 (2017).
20. J. J. Rech, L. Yan, Z. Wang, Q. Zhang, S. Bradshaw, H. Ade, and W. You, *ACS Appl. Polym. Mater.*, **3**, 30 (2020).
21. F Liu, C. Li, J. Li, C. Wang, C. Xiao, and Y Wu et al., *Chin. Chem. Lett.*, **31**, 865 (2020).
22. Y. Wang and T. Michinobu, *J. Mater. Chem. C*, **4**, 6200 (2016).
23. A. V. Akkuratov, D. K. Susarova, L. N. Inasaridze, and P. A. Troshin, *Phys. Status Solidi RRL*, **11**, 1700087 (2017).
24. A. R. Murad, A. Iraqi, S.-B. Aziz, H. Hi, S. N. Abdullah, M. A. Brza, and R. T. Abdulwahid, *Polymers*, **12**, 2910 (2020).
25. X. Gong, G. Li, S. Feng, L. Wu, Y. Liu, R. Hou, and Z. Bo, *J. Mater. Chem. C*, **5**, 937 (2017).
26. A. B. Atar, J. Y. Jeong, S. H. Han, H. Hi, and J. S. Park, *Polymer*, **153**, 95 (2018).
27. Y. A. Udum, A. Durmuş, G. E. Gunbas, and L. Toppare, *Org. Electron.*, **9**, 501 (2008).
28. E. Rustamlı, E. Goker, S. Tarkuc, Y. A. Udum, and L. Toppare, *J. Electrochem. Soc.*, **162**, G75 (2015).
29. C. H. Woo, P. M. Beaujuge, T. W. Holcombe, O. P. Lee, and J. M. Fréchet, *J. Am. Chem. Soc.*, **132**, 15547 (2010).

30. P. Piyakulawat, P. Keawprajak, A. Jiramitmongkon, M. Hanusch, J. Wlosnewski, and U. Asawapirom, *Sol. Energy Mater. Sol. Cells*, **95**, 2167 (2011).
31. Y. Qiao, X. Yin, and C. Tang, *Sci. China Chem.*, **58**, 1641 (2015).
32. H. Liu, F. Wu, B. Zhao, L. Meng, G. Wang, J. Zang, and S. Tan, *Dyes Pig.*, **120**, 44 (2015).
33. A. Islam, Z. Y. Liu, R. X. Peng, W. G. Jiang, T. Lei, W. Li, and Z. Y. Ge, *Chinese J. Polym. Sci.*, **35**, 171 (2017).
34. A. Kumar, J. G. Bokria, Z. Buyukmumcu, T. Dey, and G. A. Sotzing, *Macromolecules*, **41**, 7098 (2008).
35. P. J. Stephens, F. J. Devlin, C. F. Chabalowski, and M. J. Frisch, *J. Phys. Chem.*, **40**, 10455 (1994).
36. V. Barone and M. Cossi, *J. Phys. Chem. A*, **102**, 1995 (1998).
37. J. R. Cheeseman et al., *Gaussian 09* (Gaussian, Inc., Wallingford CT) (2009).
38. H. T. Turan, O. Kucur, B. Kahraman, S. Salman, and V. Aviyente, *Phys. Chem. Chem. Phys.*, **20**, 3581 (2018).
39. E. A. Alkan, S. Göker, H. Sarigul, E. Yildirim, Y. A. Udum, and L. Toppare, *J. Polym. Sci.*, **58**, 956 (2020).
40. S. C. Cevher, G. Hizalan, E. A. Yilmaz, D. Cevher, Y. A. Udum, L. Toppare, and A. Cırpan, *J. Polym. Sci.*, **58**, 2792 (2020).
41. J. L. Brédas, D. Beljonne, V. Coropceanu, and J. Cornil, *Chem. Rev.*, **104**, 4971 (2004).
42. B. H. Besler, K. M. Merz Jr, and P. A. Kollman, *J. Comput. Chem.*, **11**, 431 (1990).
43. H. Imoto, C. Yamazawa, S. Hayashi, M. Aono, and K. Naka, *ChemElectroChem*, **5**, 3357 (2018).
44. N. Akbasoglu, A. Balan, D. Baran, A. Cırpan, and L. Toppare, *J Polym Sci A Polym Chem*, **48**, 5603 (2010).
45. S. Göker, G. Hizalan, E. Aktaş, S. Kutkan, A. Cırpan, and L. Toppare, *New J. Chem.*, **40**, 10455 (2016).
46. D. Baran, A. Balan, S. Celebi, B. Meana Esteban, H. Neugebauer, N. S. Sarıciftci, and L. Toppare, *Chem. Mater.*, **22**, 2978 (2010).
47. G. Sonmez, H. Meng, Q. Zhang, and F. Wudl, *Adv. Funct. Mater.*, **13**, 726 (2003).